1200 V Multi-Channel Power Devices with 2.8 Ω·mm ON-Resistance

Jun Ma[*1], Catherine Erine[1], Minghua Zhu[1], Nela Luca[1], Peng Xiang[2], Kai Cheng[2] and Elison Matioli[*1]
[1]EPFL, CH-1015 Lausanne, Switzerland, [*]email: jun.ma@epfl.ch; elison.matioli@epfl.ch
[2]Enkris Semiconductor Inc., 215123 Suzhou, China

***Abstract*—**Here we report novel multi-channel AlGaN/GaN MOSHEMTs with high breakdown voltage (V_{BR}) and low ON-resistance (R_{ON}). The multi-channel structure was judiciously designed to yield a small sheet resistance (R_s) of 80 Ω/sq using only four 2DEG channels, resulting in an effective resistivity (ρ_{eff}) of only 1.1 mΩ·mm. The major limitation of high-conductivity multi-channel devices is their limited V_{BR}. This work shows that while conventional field plates (FPs) are not suited to increase V_{BR} in high-conductivity multi-channels, slanted tri-gates offer better electric field management inside the device. With a gate-to-drain separation (L_{GD}) of 15 μm, the device presented a low R_{ON} of 2.8 Ω·mm (considering the full width of the device (w_{device})) and a high V_{BR} of 1230 V, rendering a small specific R_{ON} ($R_{ON,SP}$) of 0.47 mΩ·cm^2 and an excellent figure-of-merit of 3.2 GW/cm^2. This work also shows the feasibility of E-mode multi-channel MOSHEMTs with a threshold voltage (V_{TH}) of +0.9 V at 1 μA/mm by tuning the tri-gate geometry. These results significantly outperform conventional single-channel devices and demonstrate the enormous potential of multi-channel power devices.

I. Introduction

Lateral GaN-on-Si devices are highly promising for power applications, combining high device performance and low cost, and offering a platform for advanced power integrated circuits (ICs). While GaN HEMTs are now commercially available, thanks to the remarkable progress in recent years, their performance is still much inferior to the full potential of GaN. Further advances require a major reduction in R_{ON}, while maintaining the high V_{BR} and the fast-switching capability.

The R_{ON} of high-voltage HEMTs is largely limited by the resistivity of its 2DEG channel. One approach for ultra-low R_s is to stack multiple 2DEG channels (multi-channels) [1]-[5]. This concept was first proposed in 1980s for III-Vs [1] and has led to an ultra-low R_s of 37 Ω/sq for AlN/GaN multi-channels [6], which is far below that of typical single-channel structures. However, devices based on multi-channels are still rare to date, due to the challenge in controlling all parallel channels with typical planar gate structures. Recently tri-gate structures have been shown very effective in controlling the multi-channels for normally-ON/OFF MOSHEMTs [7], for high-performance and fast-switching SBDs [8], and for RF GaN devices [9],[10]. However, to date no high-voltage device has been realized on multi-channels with R_s < 230 Ω/sq, hindering the enormous potential of multi-channel devices for power applications.

In this work we present 1200 V GaN-on-Si MOSHEMTs based on a highly-conductive multi-channel (R_s = 80 Ω/sq) using novel slanted tri-gates for a superior field management, unleashing the great potential of multi-channel power devices.

II. Epitaxy and Fabrication

The slanted tri-gate multi-channel devices (Figs. 1(a)-(c)) were fabricated based on a four-channel structure (Fig. 1(d)). The top 3 channels were formed by 20 nm $Al_{0.25}GaN$ barrier layers (Type I in Fig. 1(e)), and the bottom channel consisted of a 10 nm $Al_{0.25}GaN$ barrier (Type II in Fig. 1(f)), which were selectively doped with Si at concentrations of 1 × 10^{19} cm^{-3} and 5 × 10^{18}cm^{-3}, respectively. Such design of the multi-channels resulted in a small R_s of 80 Ω/sq, along with high N_s of 5.6 × 10^{13} cm^{-2} and mobility (μ) of 1407 cm^2·V^{-1}s^{-1}, rendering a much higher channel conductivity compared to conventional single-channel structures (Fig. 2(a)). In addition, the small R_s was achieved using only 4 channels with a small thickness of 140 nm, thanks to the heavily-doped 20 nm AlGaN barrier layers (Type I) (Fig. 2(c)), which yielded a record ρ_{eff} of 1.1 mΩ·mm (Fig. 2(b)). A thin multi-channel structure is important since it significantly simplifies the fabrication of tri-gates by reducing the aspect ratio of the fins. The bottom barrier was thinner and less doped to facilitate the control of the bottommost channel, which is the farthest from the top gate and the most prone to possible punch-through in OFF state.

In addition to fins in the gate region, the device design also contained fins in both the Source/Drain (S/D) regions, to form ohmic contact to all parallel channels. A 23 nm-thick SiO_2 gate oxide was deposited by atomic layer deposition, and the gate metals were Ni/Au. The gate region consisted of 1.5 μm-long fins, of which only 700 nm were covered by the gate. The fin width (w_{fin}) was 50 nm in the 300 nm-long tri-gate region, which increased to 100 nm at the end of the slanted tri-gate region (300 nm long), and was kept at 100 nm for the rest of its length (Figs. 1(c) and (d)). All measurements reported in this work were normalized by w_{device}.

III. Results and Discussion

The tri-gate offers a superior channel control due to its 3D architecture around the multi-channels, which is important as planar gates cannot pinch off highly conductive multi-channels (Fig. 3(a)). The planar-gate devices were in ON state even at a high V_G of -50 V, due to the large gate-to-channel distance and the shielding effect from a top channel to the ones underneath. In contrast, the tri-gate control is far more effective, resulting in a small threshold voltage (V_{TH}) of only -2.5 V for w_{fin} of 50 nm, thanks to the dominating sidewall control in narrow fins, as revealed by the peak in g_m for reduced w_{fin} in Fig. 3(a).

"© 2019 IEEE. Personal use of this material is permitted. Permission from IEEE must be obtained for all other uses, in any current or future media, including reprinting/republishing this material for advertising or promotional purposes, creating new collective works, for resale or redistribution to servers or lists, or reuse of any copyrighted component of this work in other works.

The combination of tri-gate and multi-channel structures resulted in very low R_{ON} for the MOSHEMTs. With an L_{GD} of 15 μm, the R_{ON} was only 2.8 Ω·mm (Fig. 3(b)), which is much lower than in conventional single-channel devices (Fig. 3(c)). Figure 3(c) also shows that the multi-channel structures are particularly suited to reduce the resistance in high-voltage devices, due to their large device length L, as $R_{ON} \approx R_s \cdot L/W$.

In addition to the small R_{ON}, a high V_{BR} of 1230 V was achieved using slanted tri-gates instead of conventional FPs. While FPs are essential for high V_{BR} in single-channel devices, by distributing the uneven electric field in OFF state, they are not suited for high-conductivity multi-channels. Fig. 4(a) shows deterioration of the measured V_{BR} from single-channel to multi-channel devices, despite the FP, which further decreased as R_s was reduced, and saturated at ~50 V when R_s reached 170 Ω/sq. By replacing the planar FP termination with the slanted tri-gate, the V_{BR} was greatly enhanced by 20x-fold to 1230 V, along with a small I_{OFF} below 10 μA/mm at V_D = 650 V (Fig. 4(b)). Figure 4(c) compares the V_{BR} in this work with single-channel GaN (MOS)HEMTs versus their L_{GD}, showing no degradation in V_{BR} despite the very low R_s of 80 Ω/sq, which represents a major breakthrough for high-voltage multi-channel devices.

The high V_{BR} in the multi-channel devices is due to two main reasons. Firstly, from numerical simulations we observe that planar FPs can actually diminish the V_{BR} in high-conductivity multi-channel devices. Different from single-channel devices, the multi-channels under the planar FP cannot be depleted by V_D before the high field breaks the FP, due to the high N_s, the large gate-to-channel distance, and the shielding effect previously discussed. Thus the V_{BR} is limited by the breakdown of the FP, resulting in a small constant V_{BR} of ~50 V for all types of multi-channel devices when $R_s \leq 170$ Ω/sq, regardless of their different channel and tri-gate designs (Fig. 4a). This is clearly seen from the simulated electric field distribution in multi-channel tri-gate devices with (Fig. 5) and without the planar overhanging FP (Fig. 6). High fields along z-direction were observed in the FP region and at the drain-side edges of the trenches (Fig. 5(b)), which can be greatly reduced by excluding the FP (Fig. 6(b)). Figures 5(c) and 6(c) compare the depletion length at the effective gate edge of the two devices, showing that the FP could barely deplete the planar multi-channel structure, which explains the high electric field at the FP and causes the rather small V_{BR} in devices with planar FP termination.

The second reason for the high V_{BR} is the well-distributed electric field by the slanted tri-gate [11],[12]. Since the V_{TH} in tri-gated multi-channel fins increases with narrowing fins (Fig. 3(a)), due to reduced N_s and increased gate control, a slanted w_{fin} results in a gradient of the V_{TH}, which distributes the electric field and enhances the V_{BR}. Slanted tri-gates work similarly to slant FPs, but their 3D architecture around the fin is much more suited for high-conductivity multi-channels.

Another important advantage of tri-gates for multi-channel structures is that E-mode operation was achieved by reducing the w_{fin}. Figure 7(a) shows the transfer characteristics of D- and E-mode multi-channel tri-gate MOSHEMTs fabricated on the same chip, showing a positive V_{TH} of +0.9 V at 1 μA/mm for the E-mode device, despite the high N_s of 5.6×10^{13} cm^{-2} in the multi-channel structure. This was achieved by reducing the w_{fin} to 20 nm, based on the sidewall depletion of the channels. Such normally-OFF operation can be maintained even at 150 °C (Fig. 7(b)), showing a stable small I_{OFF} of 0.3 nA/mm at V_G = 0 V. The V_{TH} can be further fine-tuned lithographically by the w_{fin} and the fin length (L_{fin}) (Fig. 7(c)), offering great flexibility for design and fabrication of GaN ICs.

Figure 8 benchmarks the slanted tri-gate multi-channel MOSHEMTs against conventional single-channel GaN (MOS)HEMTs in the literature, revealing a remarkable progress achieved in this work. Firstly, the multi-channel devices broke the limit in R_{ON} for lateral GaN power devices (Fig. 8(a)), greatly reducing the R_{ON} from ~7 Ω·mm in 600/650 V single-channel devices to 2.8 Ω·mm, while keeping a high V_{BR} of 1230 V. In addition, the multi-channel devices yielded a record figure-of-merit of 3.2 GW/cm^2 that is substantially improved from single-channel devices (Fig. 8(b)), surpassing the figure-of-merit limit for SiC, and revealing the significant potential of multi-channel devices for power applications.

IV. Conclusion

In this work we demonstrated high-voltage multi-channel MOSHEMTs using highly conductive multi-channels (R_s = 80 Ω/sq) and a slanted tri-gate structure. Low R_{ON} of 2.8 Ω·mm was achieved in addition to a high V_{BR} of 1230 V, resulting in an excellent figure-of-merit of 3.2 GW/cm^2. These results pave the path for high-voltage multi-channel devices, and can offer a platform to promote the performance of lateral power devices towards the full capabilities of GaN.

Acknowledgment

This work was supported in part by the European Research Council under grant No. 679425, in part by the Swiss National Science Foundation under grants No. PYAPP2_166901 and 200021_169362, and in part by the ECSEL Joint Undertaking under grant No. 826392.

References

[1] N H Sheng, C P Lee, R T Chen, D L Miller, and S J Lee, *IEEE Electron Device Lett.*, 6, 307-310, 1985

[2] R M Chu, Y G Zhou, J Liu, D Wang, K J Chen, and K M Lau, *IEEE Trans. Electron Device*, 53, 438-446, 2005

[3] T Palacios, A Chini, D Buttari, S Heikman, A Chakraborty, S Keller, S P DenBaars, and U K Mishra, *IEEE Trans. Electron Device*, 53, 562-565, 2006

[4] J Wei, S Liu, B Li, X Tang, Y Lu, C Liu, M Hua, Z Zhang, G Tang, and K J Chen, *IEEE Electron Device Lett.*, 36, 1287-1290, 2015

[5] H Ishida, D Shibata, H Matsuo, M Yanagihara, Y Uemoto, T Ueda, T Tanaka, and D Ueda, *2008 IEEE International Electron Devices Meeting (IEDM)*, San Francisco, CA, 2008, pp 1-4

[6] Y Cao, K Wang, G Li, T Kosel, H Xing, and D Jena, *J. Cryst. Growth*, 323, 529-533, 2011

[7] J Ma, C Erine, P Xiang, K Cheng, and E Matioli, *Appl. Phys. Lett.*, 113, 242102-1-242102-5, 2018

[8] J Ma, G Kampitsis, P Xiang, K Cheng, and E Matioli, *IEEE Electron Device Lett.*, 40, 275-278, 2018

[9] R S Howell, *et al.*, *2014 IEEE International Electron Devices Meeting (IEDM)*, San Francisco, CA, 2014, pp 11 5 1-11 5 4

[10] J Chang, S Afroz, K Nagamatsu, K Frey, S Sluru, J Merkel, S Taylor, E Steward, S Gupta, and R Howell, *IEEE Electron Device Lett.*, 40, 1048-1051, 2019

[11] J Ma and E Matioli, *IEEE Electron Device Lett.*, 38, 1305-1308, 2017

[12] J Ma and E Matioli, *Appl. Phys. Lett.*, 112, 052101-1-052101-4, 2018

"© 2019 IEEE. Personal use of this material is permitted. Permission from IEEE must be obtained for all other uses, in any current or future media, including reprinting/republishing this material for advertising or promotional purposes, creating new collective works, for resale or redistribution to servers or lists, or reuse of any copyrighted component of this work in other works.

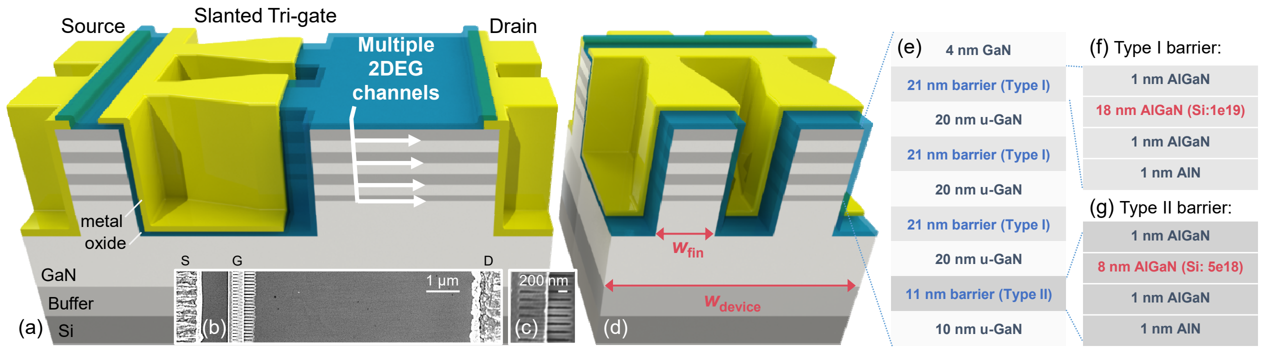

Fig. 1. (a) Schematic of the multichannel slanted tri-gate MOSHEMTs. (b) Top-view, (c) zoomed SEM images, and (d) cross-sectional schematic of the device. (e)-(g) Schematics of the multi-channel structure which contains four parallel 2DEG channels formed by two types of barrier layers.

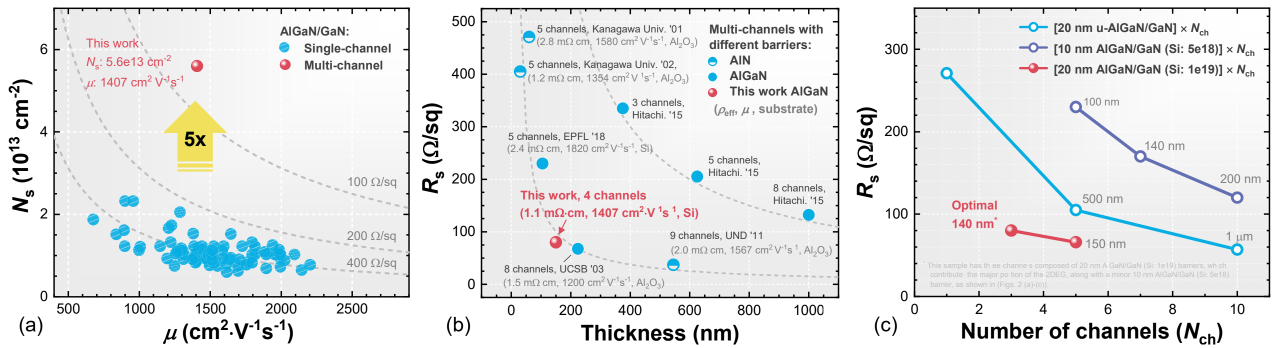

Fig. 2. (a) Comparison of N_s and μ in multi-channel and single-channel AlGaN/GaN structures. (b) Comparison of R_s and thickness of GaN multi-channel structures (more than two channels), in which the thickness of the bottommost channel layer was considered the same as the bottommost barrier layer. (c) Dependence of R_s on the number of channels (N_{ch}) in different multi-channel structures, and the numbers beside the points show the thickness of the structures.

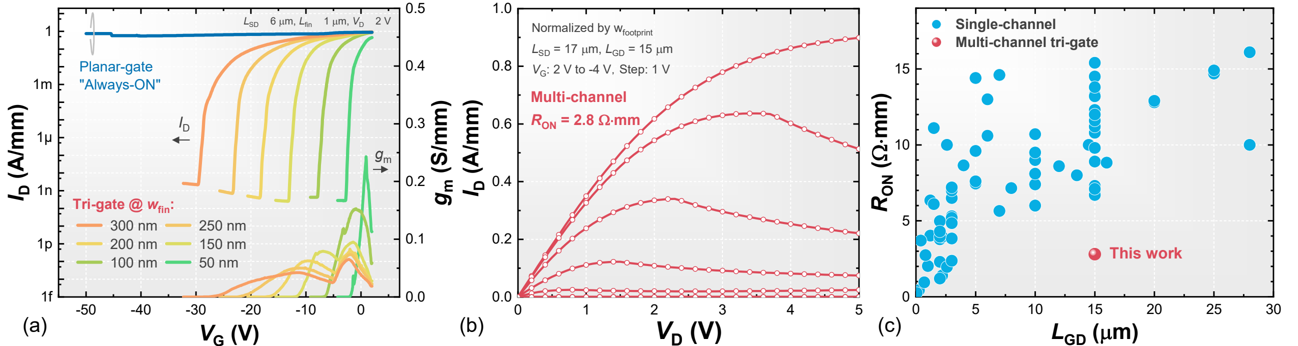

Fig. 3. (a) Transfer characteristics of multi-channel MOSHETMs based on a planar gate and on tri-gates with different w_{fin}. (b) Output characteristics of the high-voltage slanted tri-gate MOSHEMTs in this work, whose V_{TH} is -3.5 V at 1 μA/mm. (c) Comparison of R_{ON} of the slanted tri-gate multi-channel MOSHEMTs in this work and single-channel GaN (MOS)HEMTs reported in the literature (All values were normalized by the full width of the device).

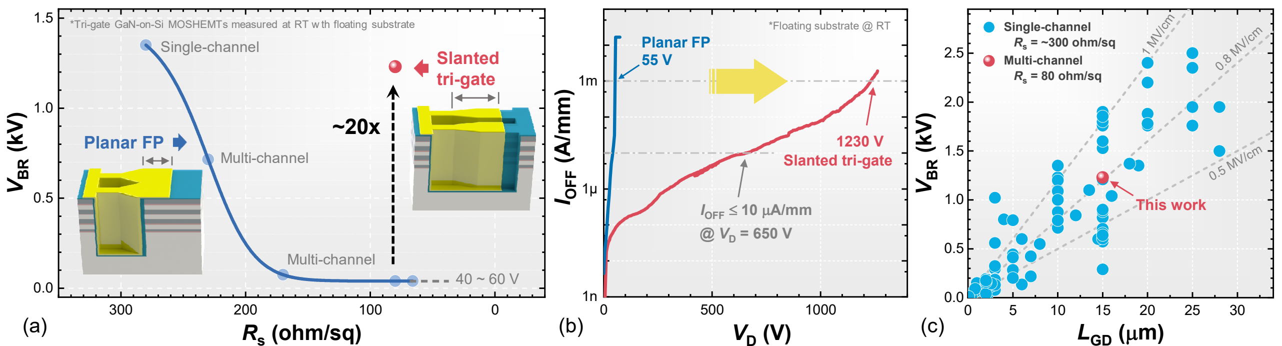

Fig. 4. (a) Dependence of V_{BR} versus the R_s in different multi-channel structures, along with the significant enhancement in V_{BR} resulted from the slanted tri-gate. (b) Comparison of OFF-state breakdown characteristics of multi-channel tri-gate MOSHEMTs with a planar FP and the slanted tri-gate. (c) Comparison of V_{BR} of the slanted tri-gate multi-channel MOSHEMTs in this work and the single-channel GaN (MOS)HEMTs reported in the literature.

"© 2019 IEEE. Personal use of this material is permitted. Permission from IEEE must be obtained for all other uses, in any current or future media, including reprinting/republishing this material for advertising or promotional purposes, creating new collective works, for resale or redistribution to servers or lists, or reuse of any copyrighted component of this work in other works.

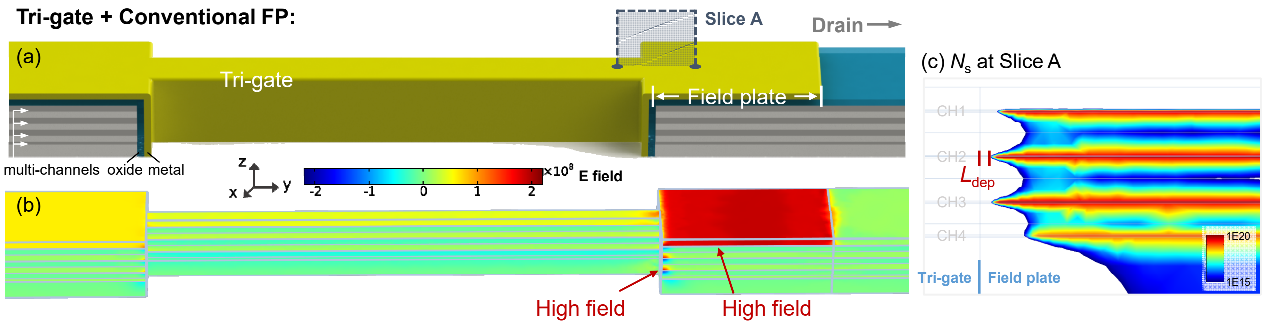

Fig. 5. (a) Schematic of the simulated tri-gate MOSHEMT with a conventional planar FP, (b) the electric field distribution in OFF state (the gate metal and oxide were not shown), and (c) the distribution of electrons close to the drain-side edge of the fin, which is the effective gate edge in this device. The V_G and V_D were -3 V and 8.5 V in the simulation, respectively, to simplify the simulation, which does not affect conclusion as the V_{BR} for such devices is very small as discussed before.

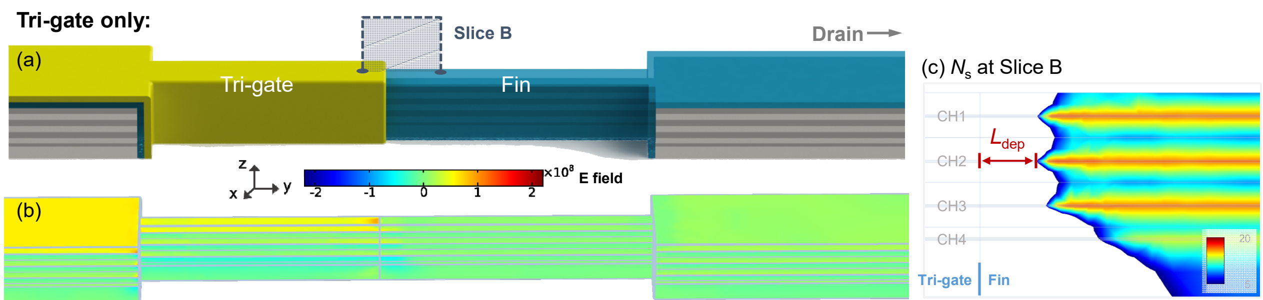

Fig. 6. (a) Schematic of the simulated tri-gate MOSHEMT with no FP, (b) the electric field distribution in OFF state (the gate metal and oxide were not shown), and (c) the distribution of electrons close to the drain-side edge of the fin, which is the effective gate edge in this device. The V_G and V_D were -3 V and 8.5 V in the simulation, respectively, to simplify the simulation, which does not affect conclusion as the V_{BR} for such devices is very small as discussed before.

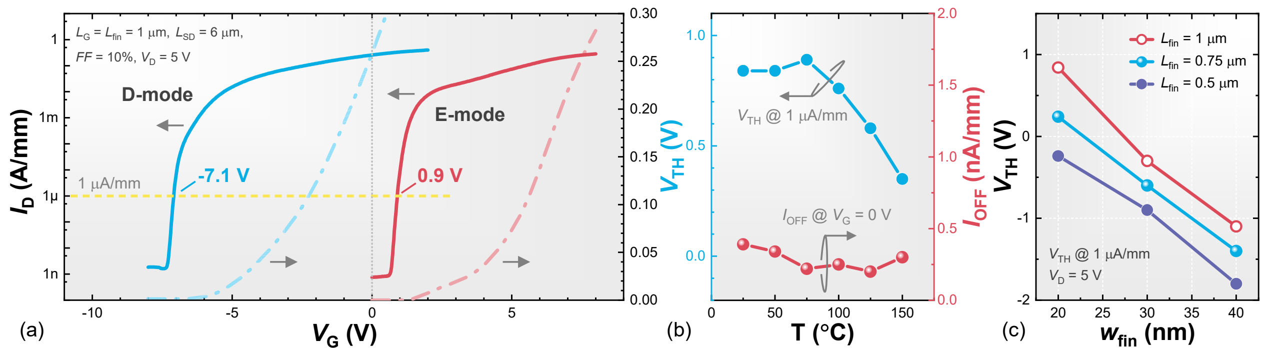

Fig. 7. (a) Transfer characteristics of E-mode and D-mode multi-channel tri-gate MOSHEMTs on the same chip by tuning the w_{fin}: 100 nm for the D-mode and 20 nm for the E-mode devices. (b) Dependence of V_{TH} and I_{OFF} of the e-mode on the temperature. (c) Dependence of the V_{TH} in multi-channel tri-gate MOSHEMTs on the w_{fin} and the length of the fins (L_{fin}).

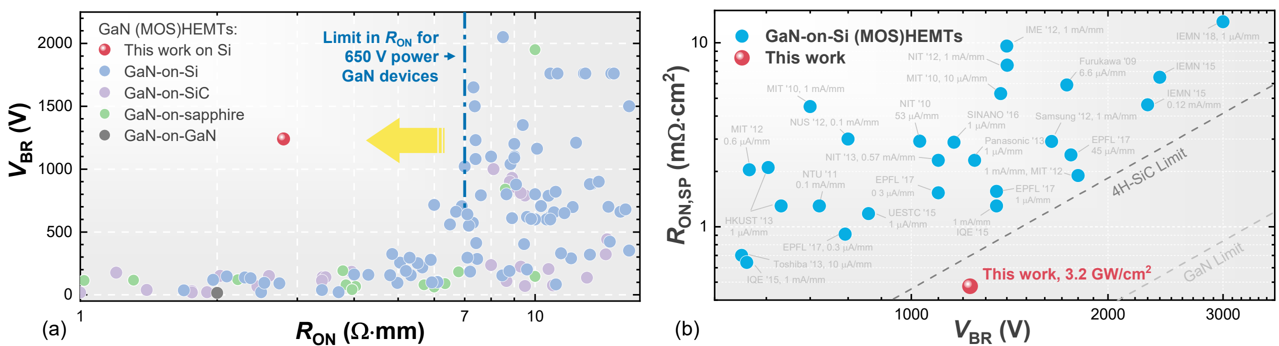

Fig. 8 (a) V_{BR} versus R_{ON} and (b) $R_{ON,SP}$ versus V_{BR} benchmarks of the slanted tri-gate multi-channel MOSHEMTs against conventional single-channel GaN (MOS)HEMTs in the literature, showing a substantial improvement by the multi-channel power devices.

"© 2019 IEEE. Personal use of this material is permitted. Permission from IEEE must be obtained for all other uses, in any current or future media, including reprinting/republishing this material for advertising or promotional purposes, creating new collective works, for resale or redistribution to servers or lists, or reuse of any copyrighted component of this work in other works.